Studies of Glycine Dimethyl Urea Crystals Grown by Aqueous Solution Method

U. Rajesh Kannan[1,*], G. Narayanasamy[2], S. Subramanian[3] and P. Selvarajan[4]
[1,*]Research Scholar, Reg. no. 12116, Department of Physics, M.D.T. Hindu College, Tirunelveli, Tamilnadu, India. *Corresponding author: rajeshphymsu@gmail.com
[2]Asso. Prof., Department of Physics, Kamaraj College, Tuticorin, Tamilnadu, India.
[3]Prof & Principal (Rtd.), Department of Physics, M.D.T. Hindu College, Tirunelveli, Tamilnadu, India.
[4]Asso. Prof., Department of Physics, Aditanar College of Arts and Science, Tiruchendur, Tamilnadu, India.
(Manonmaniam Sundaranar University, Abishekapatti, Tirunelveli, Tamilnadu, India)

Glycine dimethyl urea single crystals were grown by aqueous solution method with slow evaporation technique. Let this crystal be called as GDMU crystal. The grown crystals were characterized chemically, structurally, thermally, optically and mechanically by various studies. X-ray diffraction (XRD) analysis indicates the crystal system as monoclinic. The functional groups have been identified using Fourier transform infrared (FTIR) and FT-Raman spectral analyses. Optical transmittance studies reveal very low absorption in the entire visible region. The thermal stability of the title crystal was found by the TG/DSC analysis. Mechanical characterization was done by studying the variation of microhardness with applied load. Solubility of the material was gravimetrically analyzed. The impedance analysis was performed for the sample to understand the electrical properties. Z-scan technique was employed to confirm the third order nonlinearity of the grown crystals. Its relative SHG efficiency has been tested by Kurtz powder method and it shows 1.145 times that of potassium dihydrogen phosphate (KDP). The elements present in the sample were identified by EDAX method. Photoluminescence studies were carried out for GDMU crystal to identify the photo emission peaks and the results from the various studied were analyzed.

Keywords: Aqueous Solution method, XRD, FTIR, FT-Raman, TG/DSC analysis, Hardness, Impedance, Z-Scan Spectroscopy, Second Harmonic Generation (SHG) efficiency, EDAX, Photoluminescence.

1. INTRODUCTION

Glycine is the smallest protein-forming amino acid and is widely used in various fields owing to its different applications. The polymorphism phenomenon exhibited by glycine constitutes one of its advantageous properties [1]. Among the six different polymorphs of glycine, alpha glycine, beta glycine and gamma glycine exist under ambient conditions [2]. Combination of amino acids like glycine with organic salts are the promising materials for optical second harmonic generation and also these materials are useful in laser technology, optical communication and optical data storage technology [3]. Balakrishnan *et al.* [4] grew single crystal of glycine zinc chloride by solution method and it was studied. Ravi *et al.* [5] studied the electron paramagnetic resonance of copper ions doped glycine zinc sulphate crystals at ambient temperature. Sodium glycine nitrate,

glycine calcium dichloride, glycine calcium dibromide and glycine zinc chloride crystal structures were reported to be non-centrosymmetric [6,7,8]. The glycine sodium nitrate exhibits SHG comparable to that of potassium di phosphate (KDP) [9]. Three non-centrosymmetric glycine coordinated compounds are reported by Fleck and Bohaty [10]. Some complexes of glycine with HCl [11,12], lithium sulfate [13], H_3PO_3 [14], H_2SO_4 [15], $CaNO_3$ [16], $CoBr_2$ [17], $LiNO_3$ [18], H_2SO_4 [19,20], sodium nitrate [21], benzoyl glycine [22] form single crystals, but some of these are reported to have non linear optical (NLO) properties and some are reported not to have NLO properties. In the recent past, several researchers have reported γ-glycine single crystals using different additives such as potassium bromide [23] lithium bromide [24]. Triglycine sulfate doped with sodium bromide [25] was reported in the recent past. Urea [26] acts as a central player in crystal engineering and form many complexes and dimethyl urea form many complexes with cobalt(II) perchlorate, tetrafluoroborate and nitrate as reported by Giannis S. Papaefstathiou *et al.* [27]. In this work, a new nonlinear optical material viz. glycine dimethylurea was synthesized and single crystals were grown by slow evaporation solution growth technique at constant temperature from its aqueous solution and various studies have been carried out.

2. EXPERIMENTAL PROCEDURE

2.1. Synthesis, Solubility and Growth of the Sample

GDMU sample was prepared by dissolving analar grade glycine and N-N' diemthylurea in stoichiometric ratio 1:1 in double distilled water. The solubility of GDMU in double distilled water was determined. The Figure 1 shows the solubility curve. From the graph it is observed that the solubility increases with the temperature. In accordance with the solubility curve, the synthesized powder of GDMU was dissolved thoroughly in double distilled water at 30 ^{o}C to form saturated solution. The solution was kept in undisturbed conditions and maintained at room temperature. Transparent seed crystals were obtained after 10 days. The big sized crystals were obtained using seed immersion technique after 25 days. The harvested single crystals of the title compound are shown in Figure 2 and the grown crystals are observed to be colourless and transparent. The dimensions of the grown crystal are about 15X7X5 mm^3.

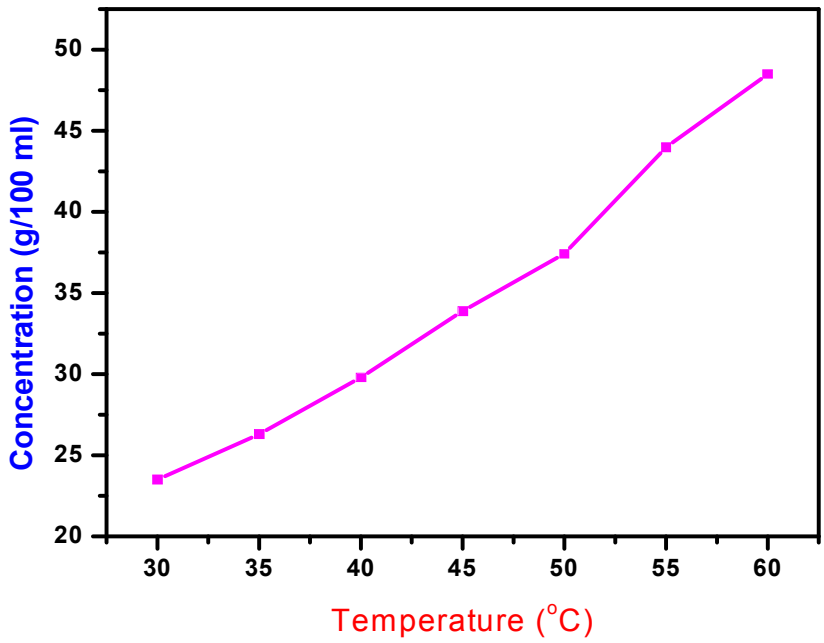

Fig. 1: Solubility curve of GDMU crystal.

Fig. 2: Photograph of the grown GDMU crystals.

2.2. Characterization Techniques

FTIR spectrum was recorded in the spectral range 400–4000 cm^{-1} using Shimadzu-8700 FTIR spectrometer and in this study the sample was in pellet form in KBr phase. Single crystal X-ray diffraction study was carried out using ENRAF NONIUS FR 590 single crystal diffractometer. The thermal analysis was carried out using Perkin-Elmer simultaneous TG/DSC analyzer. Microhardness study was carried out using SHIMADZU HMV-2T fully automated hardness tester. The UV-visible absorption spectrum was recorded using CARY 5000 instrument in the wavelength range 200 to 1000 nm. FT-Raman spectra were recorded using NEXUS670 spectrometer. UV–vis spectrum was recorded on a Perkin-Elmer Lambda 25 spectrometer in transmission mode. Second harmonic generation efficiency of the sample was determined using Kurtz powder method. Energy dispersive spectroscopy is a microanalysis technique performed in combination with Quanta 200 FEG scanning electron 101 microscope. The photoluminescence (PL) measurement was made on GDMU crystal using a Jobin Yvon-Spex spectrofluorometer with 450 W high pressure Xenon lamp as an excitation source. The PL intensity is highly dependent on the crystallinity and structural perfection of the crystal. Hence the photoluminescence studies confirm the suitability of the grown material for near violet fluorescence emission studies. The single beam Z-scan is a well known technique for measuring the degenerate nonlinearities introduced and the basic idea behind the Z-scan technique is the self-focusing or self-defocusing.

3. RESULTS AND DISCUSSION

3.1. Single Crystal X-ray Diffraction Analysis

The grown crystals of GDMU were subjected to single crystal X-ray diffraction studies using an ENRAF NONIUS CAD-4 X-ray Diffractometer with Mo-K_α radiation (λ = 0.7107 Å) to obtain the unit cell dimensions. The lattice dimensions of the grown specimen was determined from the single crystal XRD analysis using SHELX programme. From the measurement we found that the grown specimen belongs to monoclinic crystal system, having lattice dimensions: a = 5.235(7) Å, b = 13.024(6) Å, c = 5.663(4) Å, $\alpha = 90^o$, $\beta = 108.57^o$, $\gamma = 90^o$ and volume V = 366.014(5) Å.

3.2. FTIR and FT-Raman Spectral Studies

Vibrational spectroscopy is an important tool for understanding the chemical bonding and the presence of various functional groups of a material. It also provides evidence for the charge transfer interaction between the donor and acceptor groups through π–electron movement. FT-Raman spectrum will give precise resolved intensities for some unresolved bands in the FTIR spectrum [28]. FT-IR and FT-Raman spectra have been recorded for the grown crystal from 450-4000 cm^{-1} and 50-4000 cm^{-1} as shown in Figure 3 and 4, respectively. In the FTIR spectrum of grown crystal sample Figure 3, the broad absorption band from 3000 to 3500 cm^{-1} include overlap of absorption peaks due to O–H stretch of COOH and N–H stretch of NH_3^+ of glycine molecule. The CH_2 vibrations which

generally lie just below 3000 cm^{-1} are not clearly resolved in the FTIR spectrum. The broad absorption band in the above range is due to the presence of hydrogen bonding. The COO^- vibration of COOH lies around 1632 cm^{-1} and the CH_2 bending mode appears at 1333 cm^{-1} in FTIR spectrum. The torsional oscillation of NH_3^+ occurs nearly at 506 cm^{-1}. Unresolved absorption bands in the FTIR spectra are clearly resolved in the FT- Raman spectra. The FT-IR and FT-Raman assignments are given in accordance with the reported spectral data [29,30]. The observed frequencies and the tentative assignments of the Raman lines in comparison with FTIR vibrations are given in Table 1.

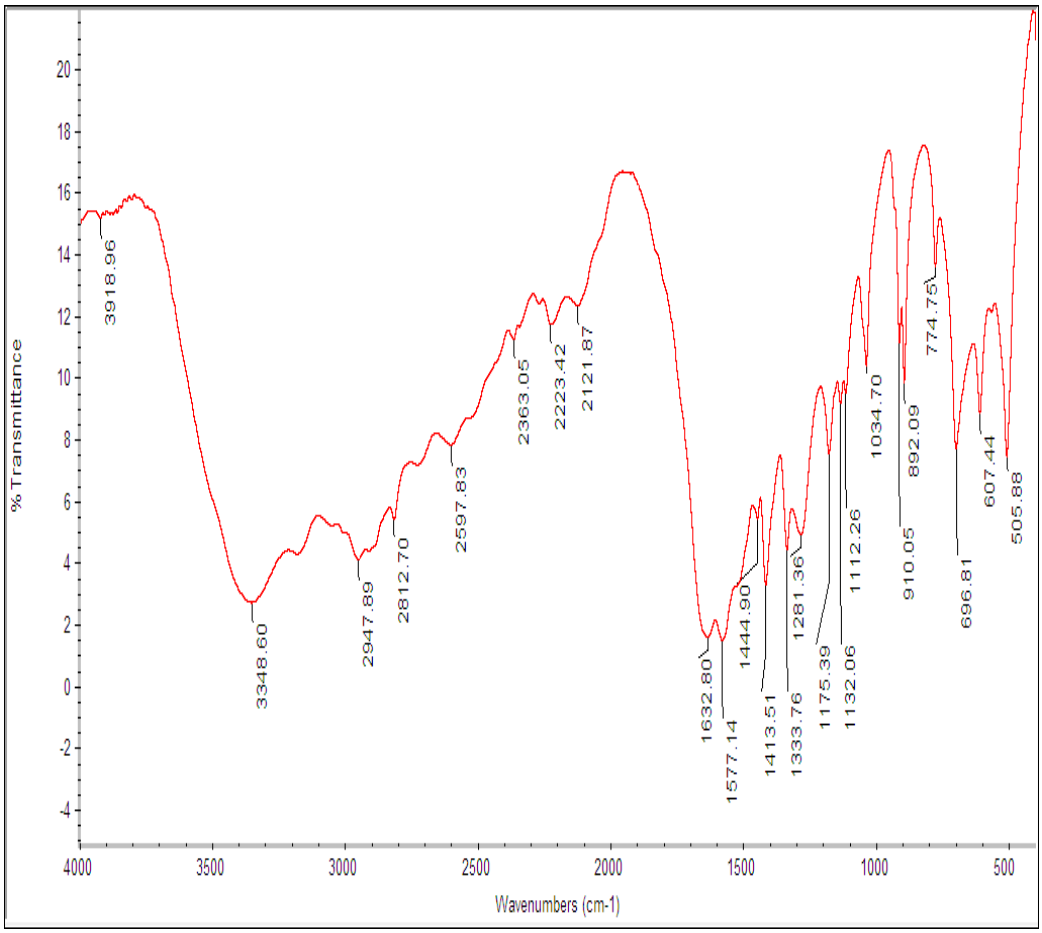

Fig. 3: FTIR spectrum of GDMU crystal.

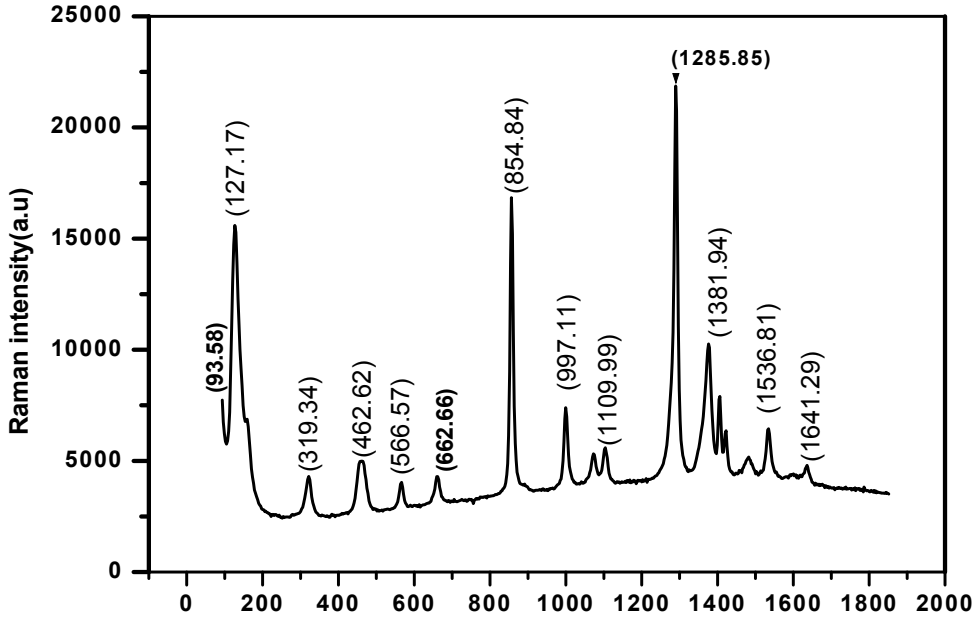

Fig. 4: FT-Raman spectrum of GDMU crystal.

Table 1: Important wave numbers observed and their assignments of FTIR and FT-Raman spectra for GDMU sample.

S. No.	FTIR (cm^{-1})	FT-Raman (cm^{-1})	Band Assignments
12	3348.60	-	N-H asymmetric stretching
3	2947.89	-	CH_2 stretching
	2363.05	-	Overtones
8	2121.87	-	Combination band
9	1632.80	1641.29	Stretching of COO^-
10	1577.14	1536	NH_2 bending
12	1413.51	-	COO^- stretching
13	1333.76	1381.94	CH_2 wagging vibration
14	1281.36	1285.85	CH_2 twisting
17	1112.26	1109.99	NH_2 deformation
19	910.06	997.11	CH_2 rocking vibration
20	892.09	854.84	CCN symmetric stretching
21	774.75	-	NH_2 bend
22	696.819	-	COO^- wagging

23	607.444	-	COO^- system bending
24	505.68		COO^- deformation
25	-	566.57	COO- in plane bending vibration
26	-	462.62	Torsional oscillation of NH_3^+
27	-	319.34	δ(CCN)
28	-	127.17	δ(CCN)
		93.58	Lattice modes

3.3. UV-Visible Spectral Studies

The optical absorption spectrum of the grown crystal has been recorded in the wavelength range of 200–800 nm at room temperature. The UV-Vis transmittance and absorbance spectra of GDMU crystal is shown in Figure 5 and 6. It is observed that the cut-off wavelength is at 240 nm and there is no absorption through the entire visible region and it is one of the most desired properties for the fabrication of optoelectronic devices. The transparent behaviour of glycine dimethylurea in the entire UV visible region is clearly illustrated by its UV-visible spectrum. The reflectance (R) of the sample is calculated using the following relation

$$R = \frac{1 \pm \sqrt{1 - e^{(\alpha d)} + e^{(\alpha d)}}}{1 + e^{(\alpha d)}}$$

where α is the linear absorption coefficient and 'd' is the thickness of the crystal. The reflectance spectrum of GDMU crystal is presented in the Figure 7 and it shows low reflectance in the entire visible region. The energy dependence of absorption coefficient suggests the occurrence of direct band gap of the crystal obeying the following relation

$$\alpha h\nu = A\sqrt{h\nu - E_g}$$

where E_g is the optical band gap energy of the crystal, h is the Planck's constant, ν is the frequency and A is a constant [31,32,33]. The plot of variation of $(\alpha h\nu)^2$ versus $h\nu$ is shown in Figure 8 and the band gap energy is calculated by extrapolation of linear part. The band gap energy is found to be 5.2 eV.

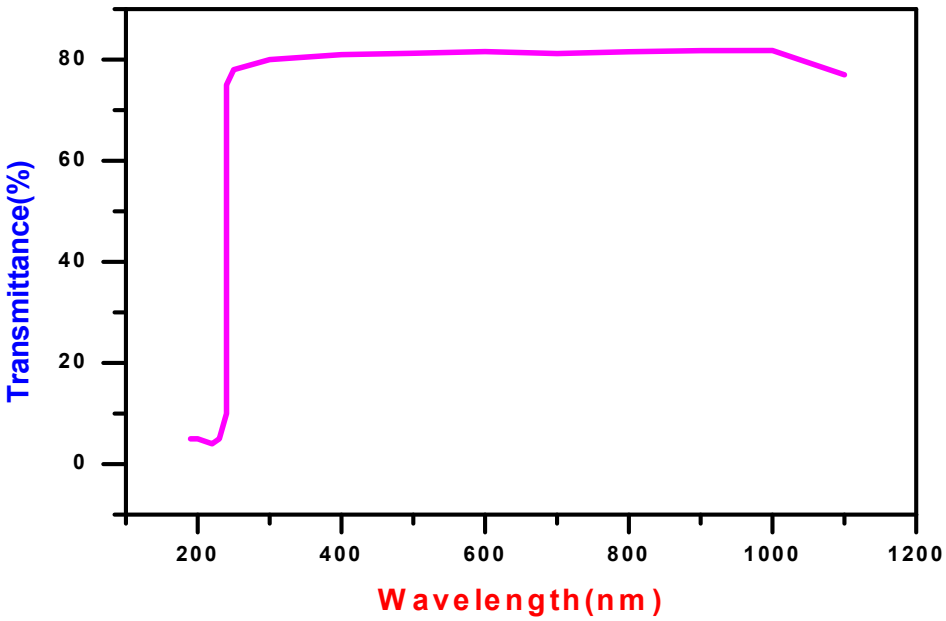

Fig. 5: UV–visible -NIR transmittance spectrum of GDMU crystal.

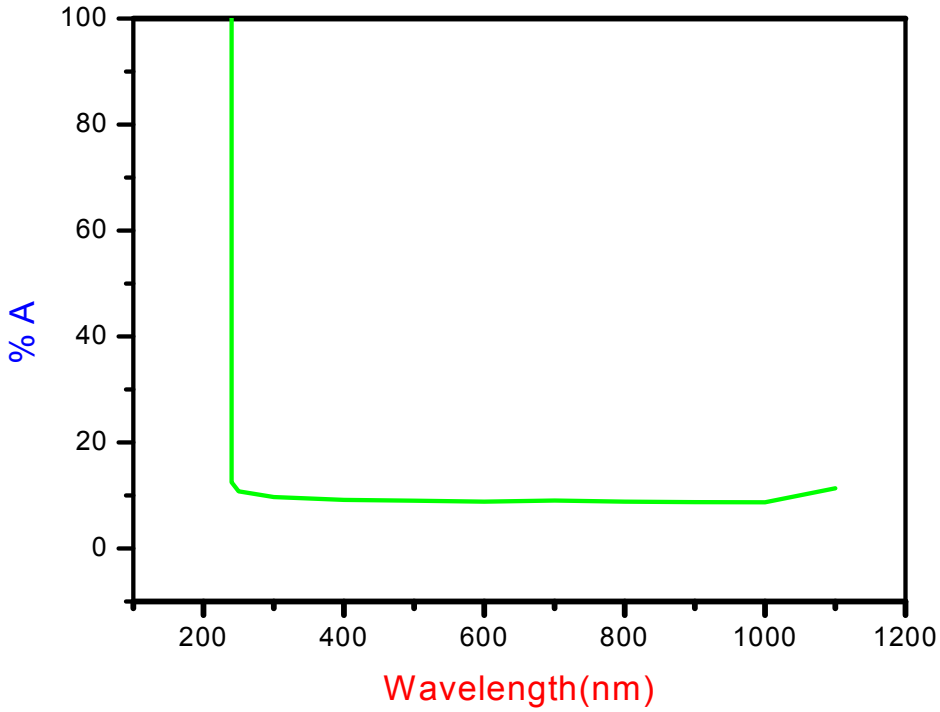

Fig. 6: UV–visible -NIR absorbance spectrum of GDMU crystal.

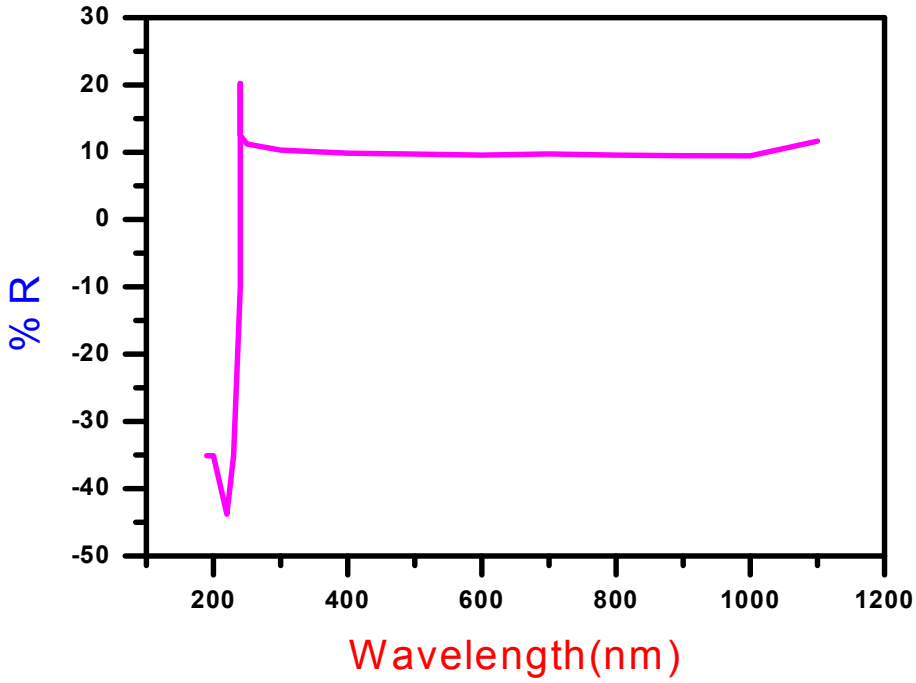

Fig. 7: UV–visible -NIR reflectance spectrum of GDMU crystal.

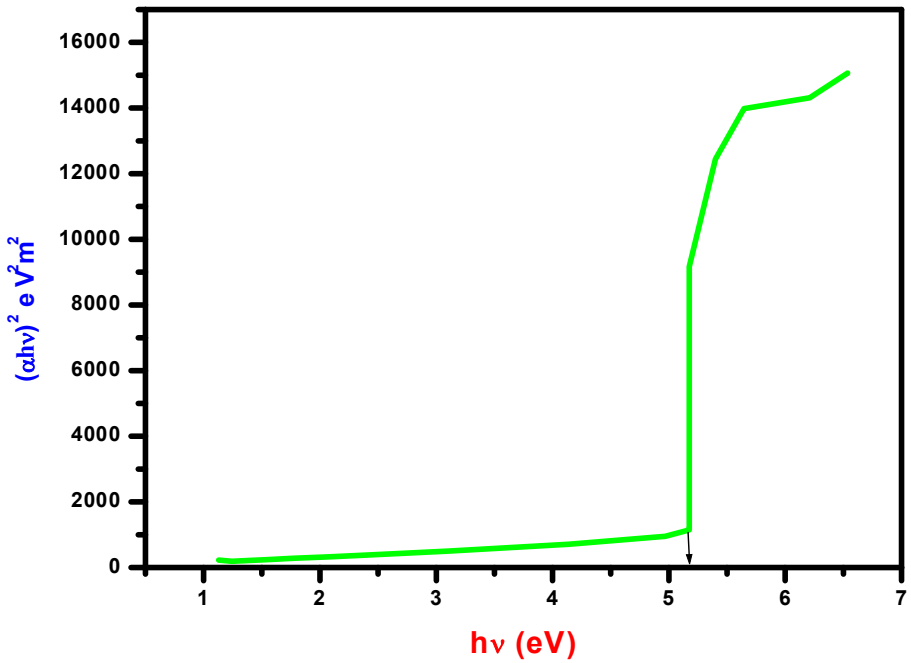

Fig. 8: UV–visible -NIR Tauc's plot of GDMU crystal.

3.4. Thermal Properties

Thermal studies are used to find the thermal stability, phase transition, endothermic and exothermic reactions that are taking place in the sample. The thermal stability of the crystal is an important factor for device fabrication. The TG/DSC analyses of GDMU crystal have been carried out between room temperature (28˚C) and 800˚C at a heating rate of 10˚C per min and recorded TG/DSC curves are shown in the Figure 9. From the TG curve, it is observed that there is no weight loss upto 150˚C and the decomposition point of the sample is noticed at 205˚C. From 200˚C to 280˚C, there is a weight loss of about 75% of the sample noticed from the results and DSC curve supports this behavior. Beyond this temperature, the further stages of decomposition of the sample have occurred as observed exothermic transition in the DSC curve. From TG/DSC studies, it is confirmed that GDMU crystal is thermally stable upto 150˚C.

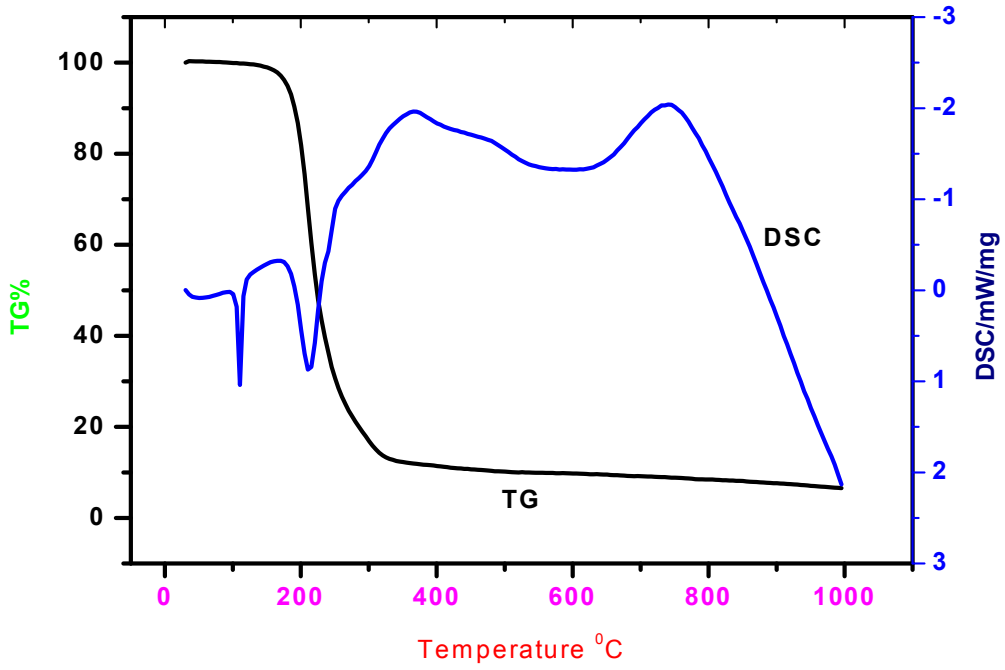

Fig. 9: TG/DSC thermal curves of GDMU crystal.

3.5. Measurement of Microhardness

Hardness is a measure of a material's resistance to localized plastic deformation. It plays a key role in device fabrication [34]. The hardness of the GDMU crystal is used for microhardness study. Before indentations, the crystal was carefully lapped and washed to avoid surface effects, which influence the hardness values. Indentations were made using a Vickers pyramidal indenter for various loads from 25 to 100 g. The measurement of the diagonal length was made at room temperature and the indentation time was 10 s. The Vickers hardness number of the crystal was calculated using the relationship H_v =

1.8544 P/d^2 where H_v is the Vickers microhardness number, P is the applied load in kg and d is the average diagonal length of the impression in mm [35]. Figure 10 shows the variation H_v versus load (P). The results show that the hardness increases with increase of the applied load and hence the sample has reverse indentation size effect. Using the Meyar's relation $P = axd^n$, the work hardening coefficient (n) can be determined. Here P is the load applied, 'a' is a constant and 'd' is the diagonal indentation length. The plot of log P versus log d is drawn and it is shown in the Figure 11 from which the value of 'n' is obtained as 2.96783. From this value it is confirmed that GDMU crystal is soft material. Stiffness constant (C_{11}) was calculated using the formula $C_{11} = H_v^{7/4}$ where H_v is the microhardness of the material. The plot of stiffness constant versus the load for the sample is presented in the Figure 12. Yield strength of the material was found using the relation $\sigma_y = H_v / 3$. The variation of yield strength with the applied load for GDMU crystal is presented in the Figure 13. From the results, it is observed that the yield strength and stiffness constant are increasing with increase in the applied load. As the values of yield strength, stiffness constant and hardness of GDMU crystal are high, the sample can be used for fabrication of NLO devices such as second harmonic generator, third harmonic generator, sum frequency generator etc.

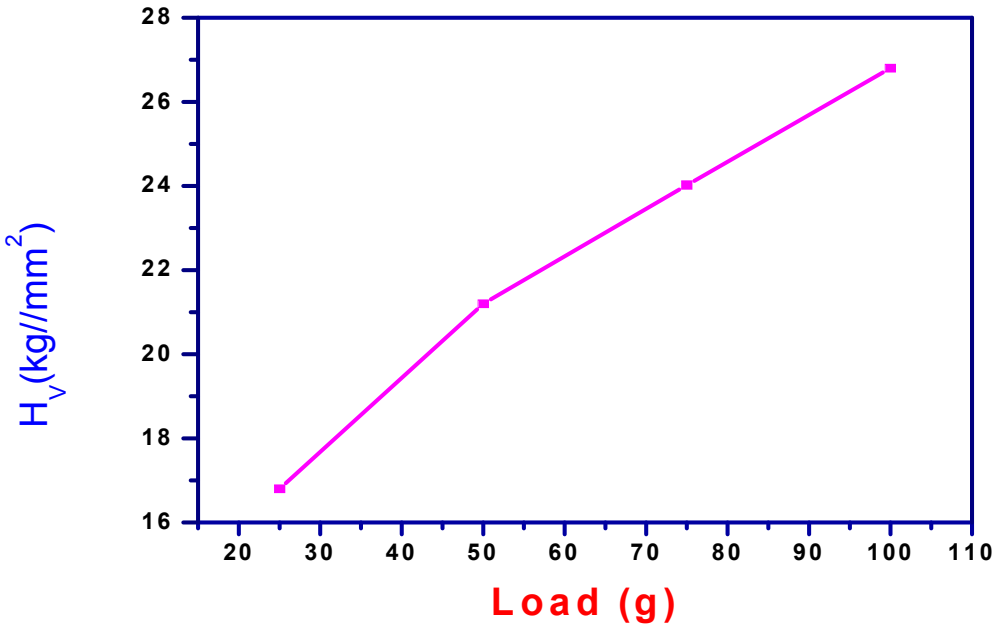

Fig. 10: Plot of Vickers hardness versus applied load for GDMU crystal.

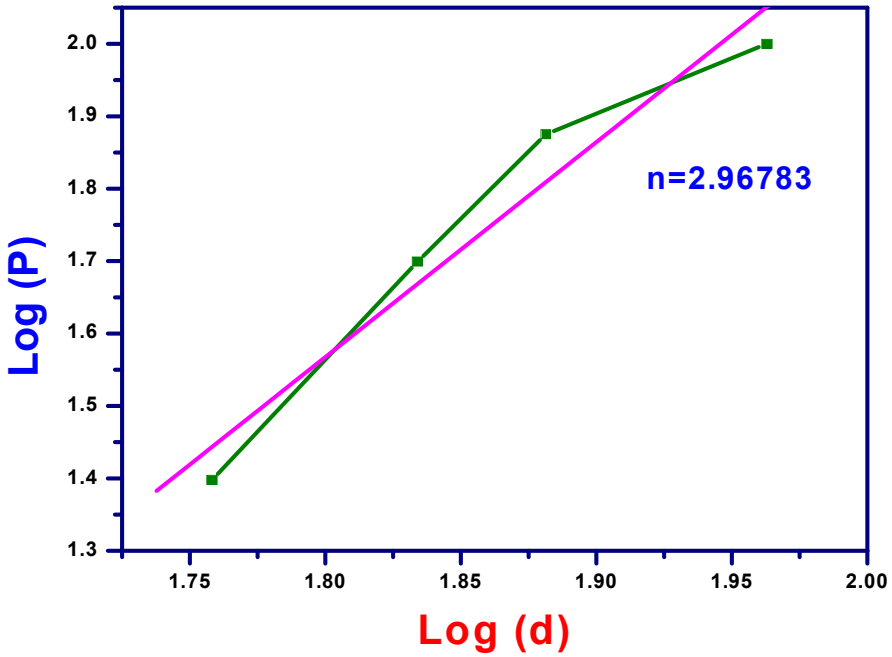

Fig. 11: Plot of log d versus log P for GDMU crystal.

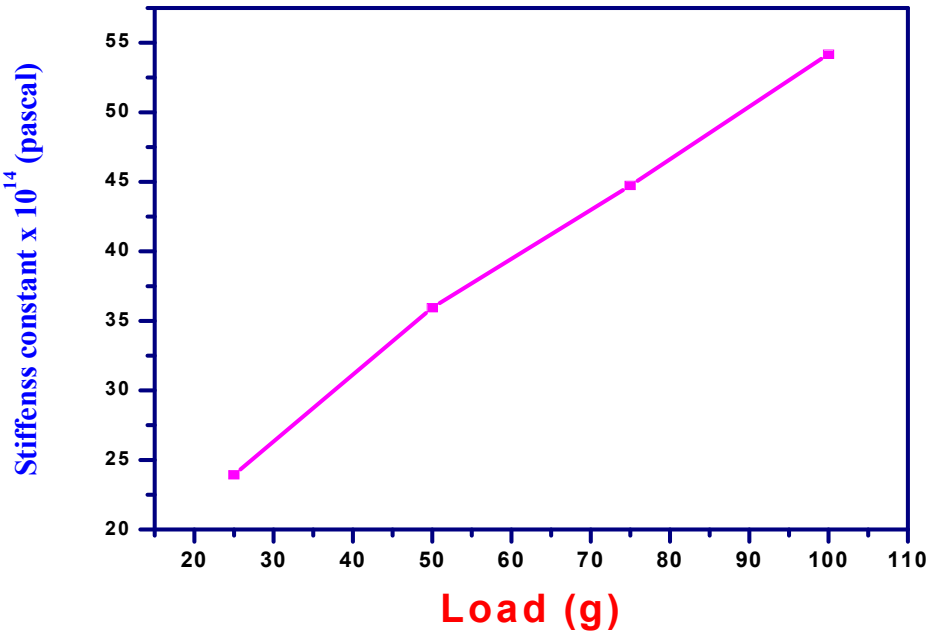

Fig. 12: Plot of stiffness constant and applied load for GDMU crystal.

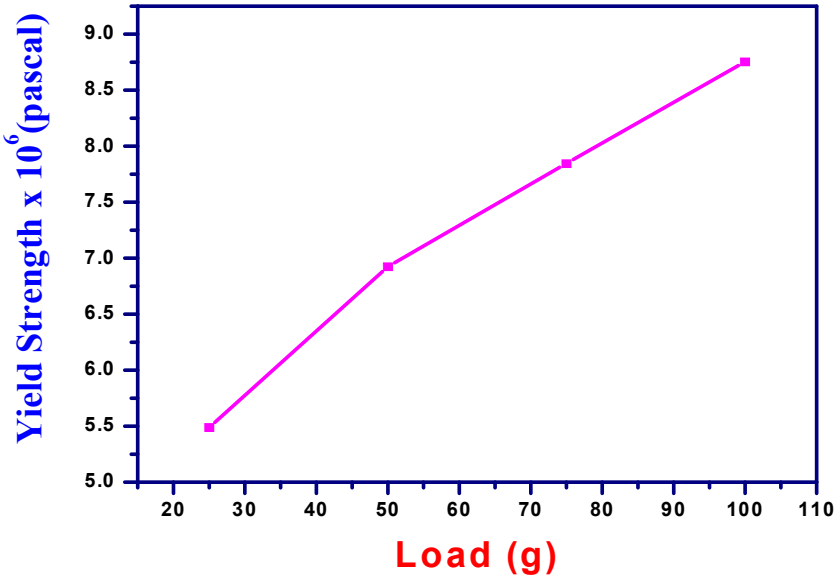

Fig. 13: Plot of yield strength versus applied load for GDMU crystal.

3.6. Second Harmonic Conversion Efficiency

The SHG conversion efficiency of GDMU crystal was determined by the modified version of the powder technique developed by Kurtz and Perry [36]. The crystal was ground into powder and densely packed between two transparent glass slides. A Nd: YAG laser beam of wavelength 1064 nm was made to fall normally on the sample cell. The green light is finally detected by the Photomultiplier tube and displayed on the oscilloscope and the second harmonic signal was detected by a photomultiplier tube and displayed on a storage oscilloscope. The second harmonics signal, generated in the crystal was confirmed from the emission of green radiation by the crystal. The input laser energy incident on the powdered sample was chosen to be 0.70 J. The results obtained for GDMU crystal is shown in the Table 2. From the results, it is found that the relative SHG efficiency of GDMU sample is 1.145 times that of the reference material (KDP).

Table 2: SHG conversion efficiency data for GDMU and KDP.

S. No.	Sample Code / Name of the Sample	Output Energy (milli joule)	Input Energy (joule)
1.	GDMU	10.21	0.70
2.	KDP (Reference)	8.91	0.70

3.7. Energy Dispersive X-ray (EDX) Analysis

Energy dispersive spectroscopy is a microanalysis technique performed in combination with Quanta 200 FEG scanning electron 101 microscope. In this investigation the title

crystal was subjected to EDX analysis to confirm the presence of elemental composition. The presence of the constituent elements in the synthesized material was confirmed by the occurrence of their respective peaks in the EDX spectrum which is shown in Figure 14. Electrons are ejected from the atoms comprising the sample's surface. The resulting electron vacancies are filled by electrons from a higher state and an X-ray is emitted to balance the energy difference between the two electrons states. The spectrum of X-ray energy versus counts is evaluated to determine the elemental composition of the sample. The EDX spectrum clearly indicates the presence of the elements such as carbon, oxygen, nitrogen in the sample.

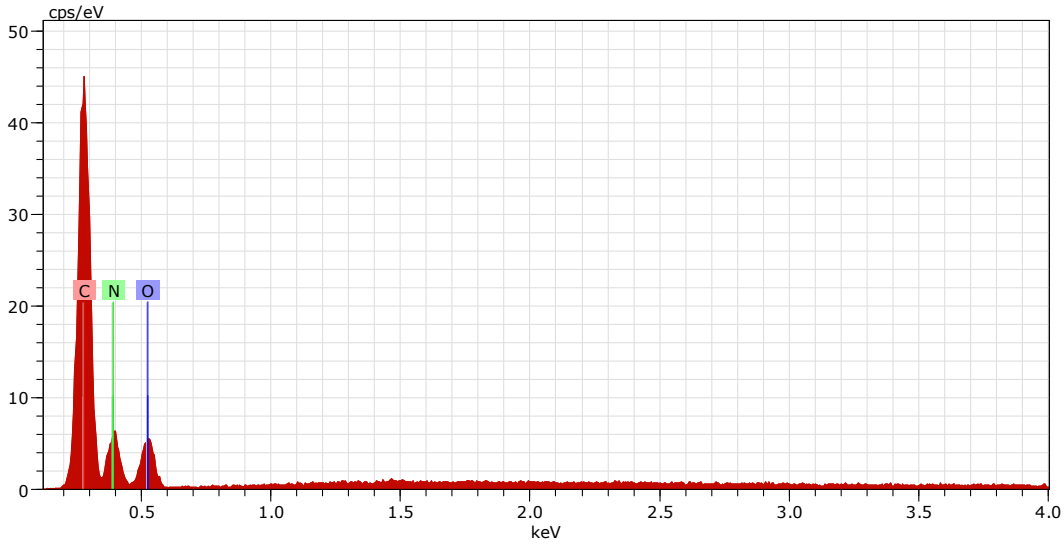

Fig.14: EDX spectrum of GDMU crystal.

3.8. Impedance Analysis

Impedance spectroscopy is a powerful technique for the characterization of electrical behaviour of the crystal. The electrical parameter such as impedance is a complex quantity and it has real part and imaginary part of impedance. Figure 15 shows the variation of the real part of impedance (Z′) with frequency at various temperatures. It is observed that the magnitude of Z′ decreases with the increase in frequency and it decreases with increase of temperature [37].

The variation of imaginary part of impedance (Z”) with frequency is presented in the Figure 16 and this value shows the relaxation behavior of the sample at different frequencies. The results show that the peak frequency (relaxation frequency) is getting shifted when the temperature of the sample increases. The Nyquist’s plot for GDMU crystal is shown in the Figure 17. The semicircles for the different temperatures could be traced, indicating the increase in conductivity of the sample. All these curves start at almost same value and the peak maxima shifts to higher values of frequency with the increase in temperature [38]. The existence of grain boundary conduction of the sample has been observed. The value of bulk resistance (R_b) and grain boundary resistance (R_g)

at different temperatures has been obtained from the intercept of the semicircular arc on the real axis (Z'). The obtained values of bulk resistance (R_b) and grain boundary resistance (R_g) of GDMU crystal are 8.25 x 10^5 ohm and 3.75 x 10^5 ohm respectively at 30°C and these values of GDMU crystal at 70°C are 4.1 x 10^5 ohm and 1.75 x 10^5 ohm respectively.

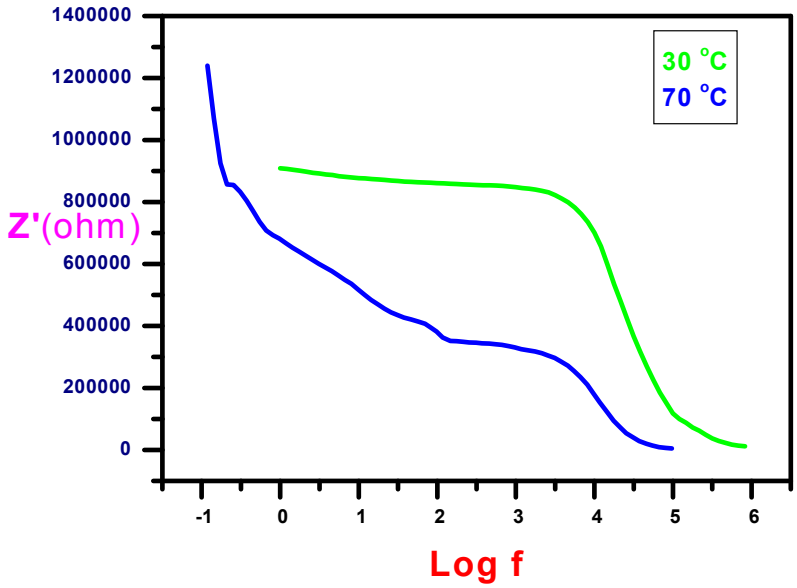

Fig. 15: Variation of real part of impedance (Z') with frequency for GDMU crystal at 30° C and 70°C.

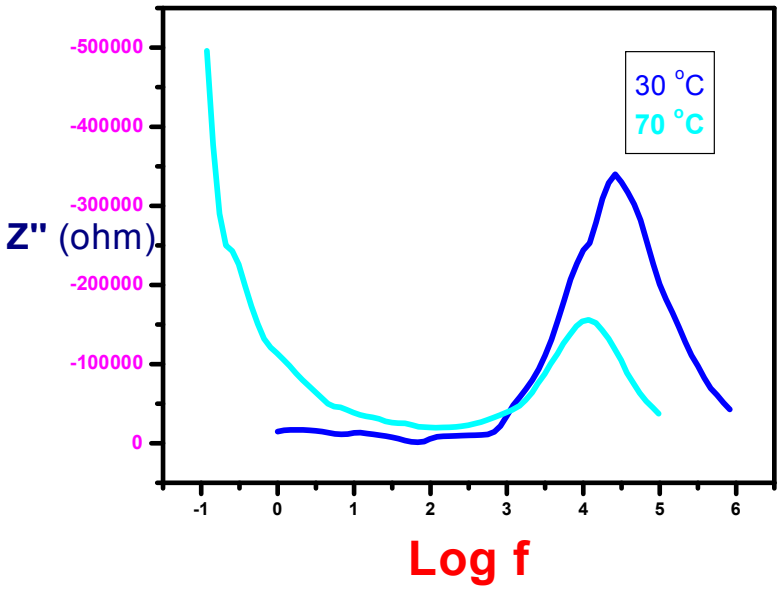

Fig. 16: Variation of imaginary part of Impedance (Z'') with frequency for GDMU crystal at 30°C and 70°C

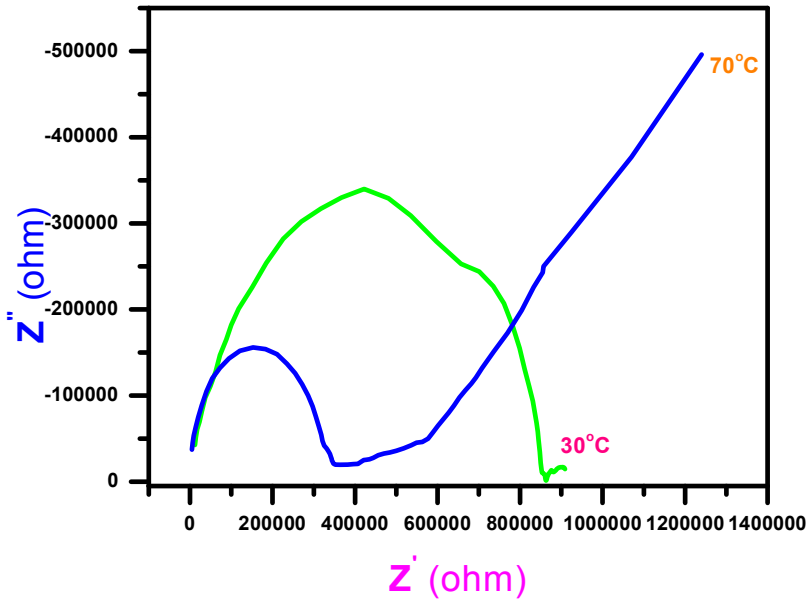

Fig. 17: Nyquist plots between Z' and Z'' for GDMU crystal at 30°C and 70°C.

3.9. Photoluminescence (PL) Studies

Photoluminescence spectroscopy is a contactless, non-destructive method of probing the electronic structure of materials. Light is directed onto a sample, where it is absorbed and imparts excess energy into the material in a process called photo-excitation. This excess energy will be dissipated by the sample through the emission of light, or luminescence. In the case of photo-excitation, this luminescence is called photoluminescence. The photoluminescence spectrum was recorded and is shown in Figure 18. The PL measurements were carried out for the excitation wavelength of 275 nm. The emission spectrum was measured in the range 300–575 nm. The strong luminescence peak at 475 nm was observed in the emission spectrum. The result indicates that the GDMU crystal has bluish green emission [39]. The PL intensity is highly dependent on the crystallinity and structural perfection of the crystal.

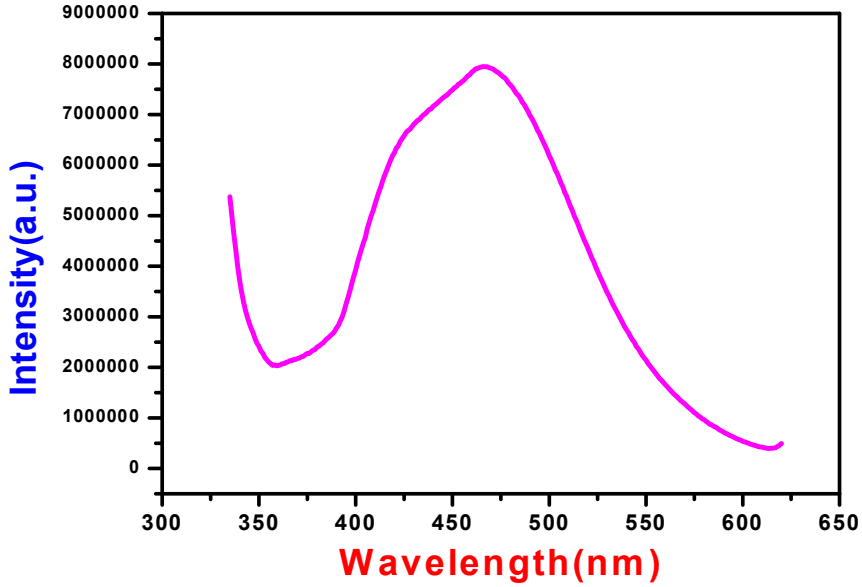

Fig. 18: Photoluminescence spectrum of GDMU crystal.

3.10. Z-Scan Measurement

The Z-scan method is a simple and popular experimental technique to measure the intensity dependent third order nonlinear susceptibility of the materials. It allows the simultaneous measurement of both the nonlinear refractive index and the nonlinear absorption coefficient. In this method, the sample is translated in the Z-direction along the axis of a focused Gaussian beam from the He-Ne laser at 632.8 nm and the far field intensity is measured as a function of the sample position. By properly monitoring the transmittance change through a small aperture at the far field position (closed aperture), one is able to determine the amplitude of the phase shift. By moving the sample through the focus and without placing an aperture at the detector (open aperture) one can measure the intensity dependent absorption of the sample [40]. When both the methods

(open and closed) are used for the measurements, the ratio of the signals determines the nonlinear refraction of the sample. The third-order nonlinear refractive index (n_2) and the nonlinear absorption coefficient (κ) of grown GDMU crystal were calculated by using Z-scan technique. The sample causes an additional focusing and defocusing depending on positive or negative values of nonlinear refractive index [41]. The open aperture and closed aperture Z-scan curves are shown in the Figures 19 and 20. Using the equations as reported in the literature [42], the third order nonlinear optical parameters are found. For GDMU crystal, the obtained values of nonlinear refractive index is -4.731×10^{-11} m^2/W, nonlinear absorption coefficient is 5.738×10^{-4} m/W and nonlinear susceptibility is 8.260×10^{-7} esu. Since the closed Z-scan curve as shown in Figure 20 shows peak to valley behavior, GDMU crystal has negative nonlinear refractive index which indicates the self-defocussing nature of the sample.

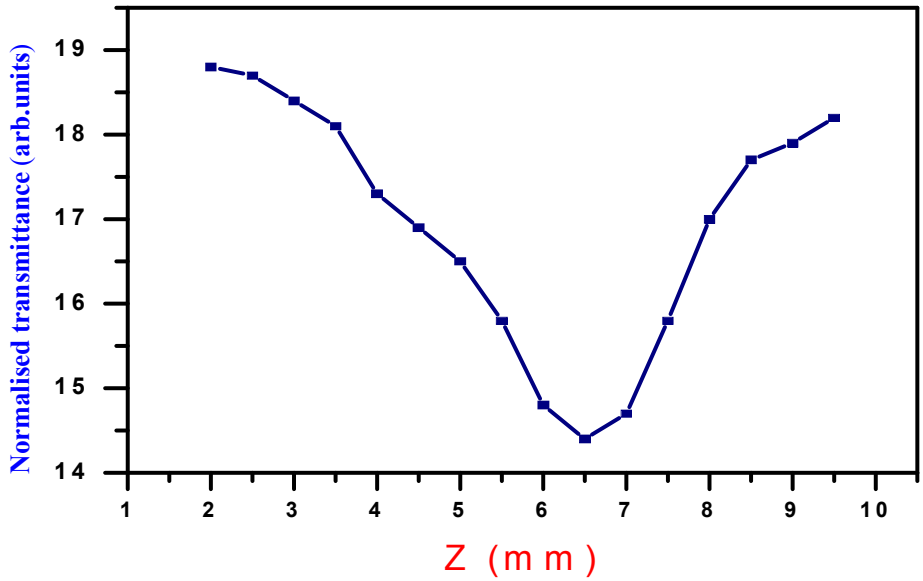

Fig. 19: Z-scan open aperture curve for GDMU crystal.

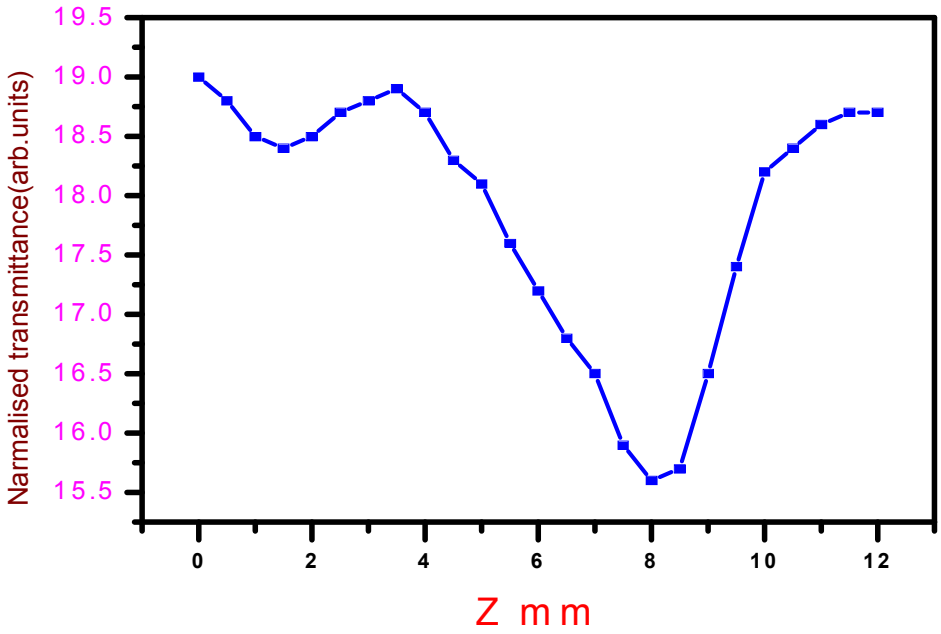

Fig. 20: Z-scan closed aperture curve for GDMU crystal.

4. CONCLUSION

Optically transparent and colourless crystals of GDMU were grown by aqueous solution method with slow evaporation technique. The crystal system and crystalline nature of the synthesized material was analyzed by single crystal XRD study. The crystal system of the sample is found to be monoclinic. The presence of various functional groups of the grown crystal was confirmed by FTIR and FT-Raman spectral analysis. UV-visible spectrum of the grown crystal shows low absorbance with cut-off wavelength at 240 nm. Bluish-green emission was observed by photoluminescence spectrum. The SHG relative efficiency of the material was found by Kurtz powder technique. Thermal stability of the grown crystal was studied by TG/DSC analysis and thermal stability of GDMU crystal is found to be upto 150^{o}C. The Vickers hardness value increases with increasing of load and other mechanical parameters such as yield strength and stiffness constant for GDMU crystal were determined. Third order nonlinear optical parameters of GDMU crystal were found by Z-scan technique. The electrical parameters such as impedance, bulk resistance and grain boundary resistance of the sample were analyzed. The various elements present in the grown crystal of GDMU were identified by EDX method.

ACKNOWLEDGEMENTS

The authors thank the staff members of SAIF, Cochin University and IIT, Chennai for the help to carry out the research work. Authors would like to thank to the staff members of St. Joseph's College, Trichy for spectral facilities, Annamalai University for TG/DSC

studies, Crescent Eng. College, Chennai for SHG test and PSN College of Technology, Tirunelveli for the impedance studies.

REFERENCES

[1] Z.H. Ansari, Y. Zeng, Y. Zhang, G.P. Demopoulos and Z. Li; "Modeling of glycine solubility in aqueous HCl–$MgCl_2$ system and its application in phase transition of glycine by changing media and supersaturation", Journal of. Crystal. Growth, Vol. 467, pp. 116-125, 2017.

[2] R.E. Vizhi and C. Yogambal; "Investigations on the growth and characterization of Y-glycine single crystal in the presence of sodium bromide", Journal of Crystal Growth, Vol.452, pp.198-203, 2016.

[3] D.S. Chemla and J. Zyss; "Nonlinear Optical Properties of Organic Molecules and Crystals", Academic Press, New York. 1987.

[4] T. Balakrishnan and K. Ramamurthi; "Structural thermal and optical properties of a semiorganic nonlinear optical single crystal: Glycine zinc sulphate", Spectrochimica Acta Part A, Vol. 628, pp. 360–363, 2006.

[5] S. Ravi and P. Subramanian; "EPR study of Cu^{2+} in glycine zinc sulphate single crystal", Solid State Communications, Vol. 143(6-7), pp. 277-279, 2007.

[6] M. Hariharan , S.S. Rajan, R. Srinivasan and S. Natarajan; "Crystal structure of a complex of glycine with zinc chloride", Z. Kristallogr., Vol. 188(1-4), pp. 217-222, 1989.

[7] R.V. Krishnakumar, M.S. Nandhini, S. Natarajan, K. Sivakumar and B. Varghese; "Glycine sodium nitrate", Acta. Crystallographica, Vol. C57, pp. 1149-1150, 2001.

[8] M.D. Aggarwal, J. Choi, W.S. Wang, K. Bhat, R.B. Lal, A.D. Shields, B. Penn, G. Benjamin and O. Donald; "Solution growth of a novel nonlinear optical material: L-histidine tetrafluoroborate", Journal of crystal Growth, Vol. 204(1), pp. 179-182, 1999.

[9] M.N. Bhat and S.M. Dharmaprakash; "New nonlinear optical material: glycine sodium nitrate", Journal of Crystal Growth, Vol. 235(1-4), pp. 511-516, 2002.

[10] M. Fleck and L. Bohaty; "Three novel non-centrosymmetric compounds of glycine: glycine lithium sulfate, glycine nickel dichloride dihydrate and glycine zinc sulfate trihydrate", Acta Crystallographica-C", Vol. C60, pp. 291-295, 2004.

[11] L.W. Hung-Wen, G.S. Yu and H.L. Strauss; "Vibrations of the Amino Group in Glycine Hydrochloride: Spectral hole Burning and Isotope Shifts", Journal. Phys. Chem. B, Vol. 102(1), pp. 298-302, 1998.

[12] B.N. Moolya and S.M. Dharmaprakash; "Nonlinear optical diglycine hydrochloride: Synthesis, crystal growth and structural characteristics", Journal of crystal growth, Vol. 293(1), pp. 86-92, 2006.

[13] M.B. Margaret, R. Sankar, S. Kalainathan, R. Jayavel and T. Irusan; "Thermal and electrical properties of Tri Glycine Sulpho Phosphate (TGSP) and L-Asparagine doped TGSP crystals", Cryst. Res. Technol., Vol. 41, pp. 712 –717, 2006.

[14] M.S. Pandian and P. Ramasamy; "Growth and characterization of solution-grown tetra glycine barium chloride (TGBC) single crystals", Journal of Crystal Growth, Vol. 310(10), pp. 2563–2568, 2008.

[15] S. Hoshino, Y. Okaya and R. Pepinsky; "Crystal structure of the ferroelectric phase of $(Glycine)_3 . H_2SO_4^{"}$, Phys. Rev., Vol. 115(2), pp. 323-330, 1959.

[16] S. Natarajan, K. Ravikumar and S.S. Rajan; "Crystal structure of diaqua nitrato glycine calcium (II) nitrate", Z. Kristallogr, Vol. 168, pp. 75-82, 1984.

[17] P. Arularasan, V. Thyanithi and R. Mohan; "Crystal growth, morphology, spectrographic characterization and thermal properties of Glycine Barium Bromo Chloride Crystals", Spectrochimica Acta Part A: Molecular and Biomolecular Spectroscopy, Vol. 144, pp. 8-16, 2015.

[18] G. Albrecht and R.B. Corey; "The Crystal Structure of Glycine", Journal of American chemical Society, Vol. 61(5), pp. 1087–1103, 1939.

[19] R. Muralidharan, R. Mohankumar, P.M. Ushasree, R. Jayavel and P. Ramasamy; " Growth and Characterization of Ainc Thiourea", J. Crystal Growth., Vol. 234, pp. 545-550, 2002.

[20] N. Balamurugan, M. Lenin, G. Bhagavannarayana and P. Ramasamy; "Growth of TGS crystals using uniaxially solution-crystallization method of Sankaranarayanan-Ramasamy", Crystal. Res. Technol, Vol. 42(2), pp.151-156, 2007.

[21] M.N. Bhat and S.M. Dharmaprakash; "New nonlinear optical material: glycine sodium nitrate", Journal of Crystal Growth, Vol. 235, pp. 511-516, 2002.

[22] H.S. Nagarajaa, V. Upadhyayaa, P.M. Rao, P.S. Aithalb and A.P. Bhat; "Organic nonlinear optical crystals of benzoyl glycine", Journal of Crystal Growth, Vol. 193(4), pp. 674-678, 1998.

[23] S.Z.A. Ahamed, G.R. Dillip, P. Raghavaiah, K. Mallikarjuna and B.D.P. Raju; "Spectroscopic and thermal studies of γ-glycine crystal grown from potassium bromide for optoelectronic applications", Arabian Journal of Chemistry, Vol. 6(4), pp. 429-433, 2013.

[24] T. Balakrishnan, R.B. Ramesh and K. Ramamurthi; "Growth, structural, optical and thermal properties of γ–glycine crystal", Spectrochimica Acta Part A: Molecular and Biomolecular Spectroscopy, Vol. 69(4), pp. 1114-1118, 2008.

[25] N.T. Shanthi, P. Selvarajan and C.K. Mahadevan; "Studies on triglycine sulfate (TGS) crystals doped with sodium bromide (NaBr) grown by solution method", Indian Journal of Science and Technology, Vol. 2(3), pp. 49-52, 2009.

[26] P.S. Corbin, S.C. Zimmerman, P.A. Thiessen, N.A. Hawryluk and T.J. Murray; "Complexation-induced unfolding of heterocyclic ureas: Simple foldamers equilibrate with multiply hydrogen-bonded sheetlike structures", Am. Chem. Soc, Vol. 123(43), pp. 10475-88, 2001.

[27] D. Balasubramanian, P. Murugakoothan and R. Jayavel; "Synthesis, growth and characterization of organic nonlinear optical bis-glycine maleate (BGM) single crystals", Journal of Crystal Growth, Vol. 312(11), pp. 1855-1859, 2010.

[28] P. Anandan, G. Parthipan, T. Saravanan, R.M. Kumar, G. Bhagavannarayana and R. Jayavel; "Crystal growth, structural and optical characterization of a semi-organic single crystal for frequnecy conversion applications", Physica B: Condensed Matter, Vol. 405(24), pp. 4951-4956, 2010.

[29] S. Sirohi and T.P. Sharma; "Bandgaps of cadmium telluride sintered film", Optical Materials, Vol. 13(2), pp. 267-269, 1999.

[30] K. Nakamoto; "Infrared and Raman Spectra of Inorganic and Coordination Compounds", John Wiley & Sons, New York, 1978.

[31] P. Yasotha, R. Thiagarajan and P. Sagunthala; "Growth Structure and Optical Studies of Undoped and Potassium Nitrate Doped Glycine Single Crystals", International Journal of Chemical and Physical Sciences, Vol. 4(6), pp. 99-104, 2015.

[32] S. Suresh and D. Arivuoil; "Synthesis, Optical and Dielectric Properties of Tris-Glycine Zinc Chloride (TGZC) Single Crystals", Journal of Minerals & Materials Characterization & Engineering, Vol. 6, pp. 517- 526, 2011.

[33] T. Mallik and T. Kar; "Optical, thermal and structural characterization of an NLO crystal, L-arginine perchlorate", Journal of Crystal. Growth, Vol. 274, pp. 251-255, 2005.

[34] B.W. Mott; "Micro Indentation Hardness Testing", Vol. 206, Butterworths, Londo, 1956.

[35] E.M. Onitsch; "The present status of testing the hardness of materials", Mikroskopie, Vol. 95(15), pp. 12-14, 1956.

[36] S.K. Kurtz and T.T. Perry; "A powder technique for the evaluation of nonlinear optical materials", Journal of Applied Physics, Vol. 39, pp. 3798–3813, 1968.

[37] A.K. Jonscher; "The Universal Dielectric Response", Nature, Vol. 267(5613), pp. 673-679, 1977.

[38] J.R. Macdonald (Eds.); "Impedance spectroscopy: Emphasizing solid materials and systems", New York: Wiley, 1987.

[39] A. Meijerink, G. Blasse and M. Glasbeek; "Photoluminescence, thermo luminescence and EPR studies on $Zn_4B_6O_{13}$", J. Phys. Condens. Matter, Vol. 2(29), pp. 6303-6313, 1990.

[40] M. Sheik-bahae, A.A. Said and E.W. Van Stryland; "High-sensitivity, single-beam n_2 measurements", Optics letters, Vol. 14(17), pp. 955-957, 1989.

[41] M. Sheik-Bahae, A.A. Said and E.W. Van Stryland; "High-sensitivity, single beam n_2 measurements", Opt. Lett, Vol. 14(17), pp. 955-957, 1989.

[42] N. Rathna, V.S. John, T. Chithambarathanu and P. Selvarajan; "Growth, NLO, Z-scan and impedance studies of glycine potassium sulphate crystals grown by aqueous solution technique", Journal of Chemical and Pharmaceutical Research, Vol. 8(5), pp. 177-185, 2016.